

# DiffOp-net: A Differential Operator-based Fully Convolutional Network for Unsupervised Deformable Image Registration

Jiong Wu

J. Crayton Pruitt Family Department of Biomedical Engineering, University of Florida, Gainesville, FL, USA

**Abstract.** Existing unsupervised deformable image registration methods usually rely on metrics applied to the gradients of predicted displacement or velocity fields as a regularization term to ensure transformation smoothness, which potentially limits registration accuracy. In this study, we propose a novel approach to enhance unsupervised deformable image registration by introducing a new differential operator into the registration framework. This operator, acting on the velocity field and mapping it to a dual space, ensures the smoothness of the velocity field during optimization, facilitating accurate deformable registration. In addition, to tackle the challenge of capturing large deformations inside image pairs, we introduce a Cross-Coordinate Attention module (CCA) and embed it into a proposed Fully Convolutional Networks (FCNs)-based multi-resolution registration architecture. Evaluation experiments are conducted on two magnetic resonance imaging (MRI) datasets. Compared to various state-of-the-art registration approaches, including a traditional algorithm and three representative unsupervised learning-based methods, our method achieves superior accuracies, maintaining desirable diffeomorphic properties, and exhibiting promising registration speed.

**Keywords:** Deformable image registration · Unsupervised learning · Differential operator · Cross-coordinate attention · Fully convolutional network

## 1 Introduction

Deformable image registration is a crucial step in numerous medical image applications, addressing the inherent variations in anatomical structures due to differences in subjects, scan times, or scanners. This process is integral for tasks such as disease diagnosis, treatment planning, and monitoring, aiming to establish a deformation field that aligns voxels in moving images with those in the fixed image [29,18,24]. Over the past decades, a diverse array of deformable image registration methods has been developed [3,1,26]. Initially, methodologies often relied on physical models, solving the registration problem by minimizing energy functions. These approaches, despite their effectiveness, were limited

by their computational complexity and the vast degrees of freedom within the solution space, resulting in significant processing times [28,31].

With the advancements in deep learning, particularly the integration of Fully Convolutional Networks (FCNs) into computer vision tasks, FCNs have been adapted for deformable image registration. This adaptation has led to significant reductions in registration time [30,7,10]. In the context of deformable registration, two primary approaches have emerged: supervised and unsupervised learning-based methods [30,8,12,20,25]. Supervised methods utilize ground truth displacement fields or segmentation maps to guide parameter learning, whereas unsupervised methods optimize FCNs directly using predefined loss functions, eliminating the need for ground truth data. Given the challenges in acquiring ground truth displacement fields and segmentation maps, current research predominantly focuses on unsupervised deformable registration methods.

In unsupervised deformable registration frameworks, the selection of loss function plays a critical role in determining performance. Typically, the loss function comprises terms for assessing image similarity and ensuring smoothness in the predicted displacement field [2,14,4]. Despite achieving promising results, existing methods struggle with preserving the topology of warped moving images, which is crucial for downstream tasks. To tackle this issue, several studies have incorporated stationary velocity field-based systems (SVF) into their registration architectures, enhancing the smoothness of the displacement field [7,13]. Furthermore, some approaches have employed Jacobian determinant regularization on the displacement field to improve topology preservation [19,17]. Despite the integration of powerful self-attention neural networks like Transformers [5,6], registration accuracy remains constrained.

Inspired by traditional diffeomorphic image registration methods, specifically the large deformation diffeomorphic metric mapping (LDDMM) [3,28], we introduce a novel framework named DiffOp-net. This framework aims to address the existing gaps in registration accuracy while maintaining desirable diffeomorphic properties. Our contributions are as follows:

- We introduce a differential operator into the unsupervised deformable registration framework, ensuring precision registration while preserving diffeomorphic properties.
- Our model enables the handling of large deformations in image pairs by employing a multi-resolution framework based on the smoothness of the velocity field.
- A cross-coordinate attention module (CCA) is proposed to further capture large deformation and thus enhance registration performance.

## 2 Methods

### 2.1 Deformable Image Registration

Given an image pair, a moving image  $M$  and a fixed image  $F$ , defined on the background space  $\Omega \in \mathbb{R}^3$  with the same size of  $n_x \times n_y \times n_z$ . The goal of

the deformable image registration is to determine a deformation field  $\phi : \Omega \rightarrow \Omega$ , such that  $\phi(M)$  is well aligned to  $F$ . In our registration framework, the deformation field  $\phi$  is defined through the following ordinary differential equation (ODE)

$$\frac{d\phi_t}{dt} = v(\phi_t), \quad (1)$$

where  $\phi_0 = id$  denotes the identity mapping such that  $id(x) = x$ ,  $x \in \Omega$ ,  $v$  denotes stationary velocity field and can be integrated over  $t = [0, 1]$  to obtain the final transformation  $\phi_1$ .

## 2.2 Differential Operator Embedding and Backpropagation

In an unsupervised learning-based deformable image registration framework, neural networks are trained by using predefined loss functions. Let  $\theta$  be the parameters of neural network, loss function  $\mathcal{J}_\theta$  has the following form

$$\mathcal{J}_\theta(\phi; M, F) = \mathcal{S}(\phi(M), F) + \lambda \mathcal{R}(\phi), \quad (2)$$

where  $\mathcal{S}$  is a matching term used to evaluate the similarity between the  $\phi(M)$  and the  $F$ ,  $\mathcal{R}$  is a regularizer to drive the optimization towards a solution that satisfied some specific properties and  $\lambda$  is a hyperparameter to balance the matching term  $\mathcal{S}$  and regularizer  $\mathcal{R}$ . A widely used regularizer is the diffusion regularizer  $\mathcal{R} = \|\nabla \phi\|^2$ , where  $\nabla$  denotes the nabla operator. To further improve the registration performance, other studies construct a registration framework based on SVF, the regularizer of  $\mathcal{R}$  directly acts on the velocity field with the form of  $\mathcal{R} = \|\nabla v\|^2$ . The optimization towards generating a sufficient smooth velocity field can be integrated to obtain a displacement field with diffeomorphic properties. Despite the larger  $\lambda$  results in a much smoother displacement field, the registration accuracy will be largely reduced.

To tackle this problem, inspired by the traditional LDDMM algorithm [3,28], we introduce a differential operator  $\mathcal{L}$  into the proposed registration framework which with the following form

$$\mathcal{L} = -\gamma \nabla^2 + Id, \quad (3)$$

where  $\nabla^2$  is the Laplacian operator,  $Id$  is the identity operator, and the hyperparameter  $\alpha > 0$  determines the smoothness of  $v$ , the larger the value of  $\gamma$  the smoother of the velocity field. After embedding  $\mathcal{L}$  into the loss function  $\mathcal{J}_\theta$ , the form of  $\mathcal{J}_\theta$  can be derived as

$$\mathcal{J}_\theta(\phi; M, F) = \mathcal{S}(\phi(M), F) + \lambda \int_0^1 \|\mathcal{L}v\|_{\mathcal{L}^2}^2 dt. \quad (4)$$

We can note from LDDMM [3] that  $\mathcal{L}$  is a positive-definite symmetric differential operator acting on the velocity field  $v \in V$  ( $V$  denotes a tangent space of diffeomorphisms  $\phi$ ) and mapping  $v$  into a dual space  $V^*$  making Eq. (4) is calculated in the dual space  $V^*$ .

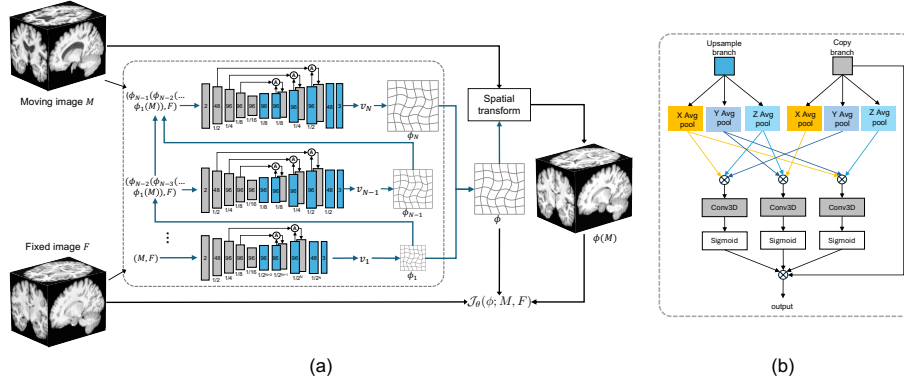


**Fig. 1.** (a) Architecture of the proposed differential operator-based multi-resolution deformable registration framework (DiffOp-net); (b) Architecture of the cross-coordinate attention module (CCA).

Due to the velocity field  $v$  defined and predicted in the original space  $V$ , hence the gradient of the loss function  $\nabla \mathcal{J}_\theta$  should be calculated and transferred from  $V^*$  to  $V$  to realize its backpropagation in the original space. It can be implemented by using the dual operator  $\mathcal{K} = (\mathcal{L}^\dagger \mathcal{L})^{-1}$ , where  $\mathcal{L}^\dagger$  is adjoint of  $\mathcal{L}$ . Therefore the gradient of the loss function is calculated as

$$\nabla \mathcal{J}_\theta(\phi; M, F) = -\mathcal{K}(\partial \mathcal{S}(\phi(M), F) \cdot \nabla \phi(M)) + \lambda v, \quad (5)$$

where  $\nabla \phi(M)$  denotes the gradient of  $\phi(M)$  and  $\partial \mathcal{S}(\phi(M), F)$  denotes the Gateaux derivative of  $\mathcal{S}(\phi(M), F)$ . In this paper, we set the  $\mathcal{S}$  to be the negative of normalized cross-correlation (NCC).

### 2.3 Registration Framework

The left panel of Figure 1 illustrates the architecture of the proposed differential operator-based multi-resolution deformable registration framework (DiffOp-net). It consists of  $N$  different levels generate  $N$  velocity fields with the resolutions gradually increased by times of 2. After integration steps,  $N$  different displacement fields  $\{\phi_1, \phi_2, \dots, \phi_N\}$  are obtained by integrating the corresponding velocity fields over  $t \in [0, 1]$ . Then the final displacement field  $\phi$  is calculated by combining  $\phi_i$  ( $i = 1, 2, \dots, N$ ) together. After applying  $\phi$  on the moving image  $M$ , we will obtain the warped transformed moving image  $\phi(M)$ . Since the hyperparameter  $\gamma$  controls the smoothness of the predicted velocity fields and the registration process in lower resolution will capture more global information for large deformation, therefore we proposed a novel registration strategy via embedding the different values of  $\gamma$  in  $N$  levels to construct a coarse-to-fine registration pipeline to enhance the framework captures large deformation in image pairs.

We adopt  $N$  FCNs with each one similar to the 3D UNet architecture to predict the velocity fields. As shown in the left panel of Figure 1, each FCN

consists of an encoder and a decoder. To simplify the architecture, we set  $N$  to 3 in this study. The encoder architecture at different levels is the same, i.e. the inputted image pairs are firstly convolved by  $C$  convolutional filters. Then the number of filters is fixed to  $2C$  in the following 3 convolutional layers (DiffOp-net with  $C = 48$  as the default setting). We set the kernel size to  $3 \times 3 \times 3$  for each convolutional layer to limit the parameters and set the value of stride in each dimension to 2 to downsample the size of the feature maps. In terms of the decoder, deconvolution operations are adopted to upsample the feature maps to reach the desired resolution for the velocity fields in the specific levels. Skip connections are added in each FCN to propagate the information from the earlier layers to the deeper ones.

## 2.4 Cross-coordinate Attention Module

To date, attention modules such as squeeze-and-excitation (SE) [11], BAM [22], and CBAM [27] are widely used in computer vision tasks and introduced into deformable image registration. However, only local relations are captured limiting the registration accuracy. In addition, although some other studies proposed cross-attention mechanisms to improve registration performance, higher computational complexity and memory consumption resulted in longer alignment time and a limited application environment [6,23]. To alleviate the aforementioned issues, we proposed a novel efficient cross-coordinate attention module (CCA) to model long-range dependencies inside image pairs in registration.

As shown in the right panel of Figure 1, CCA embedded in skip connections taking the outputs of the copying branch (denoted as  $\mathbf{X}_{cop} \in \mathbb{R}^{C \times H \times W \times D}$ ) and the outputs of decoder layer (denoted as  $\mathbf{X}_{up} \in \mathbb{R}^{C \times H \times W \times D}$ ) as inputs. Then three 1D global average pooling operations respectively aggregate  $\mathbf{X}_{cop}$  and  $\mathbf{X}_{up}$  along the three axes directions into three separate directionaware feature maps  $\mathbf{z}_{cop/up}^{h,w}$ ,  $\mathbf{z}_{cop/up}^{h,d}$  and  $\mathbf{z}_{cop/up}^{w,d}$  followed by the cross multiplication between a specific direction of the upsampling branch and the other two directions of the copying branch. After three 3D convolutional operations and *Sigmoid* functions, feature maps are integrated and used as attention weights on feature maps  $\mathbf{X}_{cop}$ . Finally, the output  $\mathbf{Y}$  of our CCA module can be written as

$$\begin{aligned} \mathbf{Y} = & \mathbf{X}_{cop} \times \sigma \left( F \left( \mathbf{z}_{cop}^{h,w} \times \mathbf{z}_{cop}^{h,d} \times \mathbf{z}_{up}^{w,d} \right) \right) \times \sigma \left( F \left( \mathbf{z}_{cop}^{h,w} \times \mathbf{z}_{up}^{h,d} \times \mathbf{z}_{cop}^{w,d} \right) \right) \\ & \times \sigma \left( F \left( \mathbf{z}_{up}^{h,w} \times \mathbf{z}_{cop}^{h,d} \times \mathbf{z}_{cop}^{w,d} \right) \right), \end{aligned} \quad (6)$$

where  $\mathbf{z}_{cop/up}^{h,w} = \frac{1}{D} \sum_{i=1}^D \mathbf{X}_{cop/up}(h, w, i)$ ,  $\mathbf{z}_{cop/up}^{h,d} = \frac{1}{W} \sum_{j=1}^W \mathbf{X}_{cop/up}(h, j, d)$ ,  $\mathbf{z}_{cop/up}^{w,d} = \frac{1}{H} \sum_{k=1}^H \mathbf{X}_{cop/up}(k, w, d)$ ,  $\sigma$  denotes the *Sigmoid* function and  $F$  denotes the 3D convolutional operation with the kernel size of  $1 \times 1 \times 1$ .

## 2.5 Implementation Details

FCNs and the proposed CCA module in the proposed DiffOp-net were implemented based on the Pytorch platform. Because of lacking Autograd mechanism

for the operators  $\mathcal{L}$  and  $\mathcal{K}$  in Pytorch, we first implemented all components of the loss function  $\mathcal{J}_\theta$  and the corresponding gradient  $\nabla \mathcal{J}_\theta$  using CUDA and then integrated them into Pytorch framework to realize the parameters learning in forward and backward propagations. Besides, to balance the registration accuracy and the smoothness of predicted velocity fields as well as to enhance the capturing large deformation in image pairs, we empirically set the window size to 9 to calculate NCC, the value of  $\lambda$  to  $1 \times 10^6$  and the values of  $\gamma$  to 0.005, 0.002 and 0.001 respectively in the three registration levels. Three FCNs were trained simultaneously to reach a globally optimal solution by utilizing *Adam* with the learning rate of  $1 \times 10^{-4}$  and the batch size of 1. The source code is available at [https://github.com/\\*](https://github.com/*).

### 3 Experiments

#### 3.1 Experimental Setting

**Dataset:** To evaluate the performance of the proposed method, three publicly available T1-weighted magnetic resonance imaging (MRI) datasets with one for training and another two for evaluation were utilized. The training dataset consists of 506 images from the ADNI 1 cohort dataset [21] wherein 500 images are randomly selected for training and the remaining 6 images yield 5 pairs registration for validation. We employ the MICCAI 2012 Multi-Atlas Labelling Challenge dataset (MALC) [16] containing 35 MRIs and the Mindboggle101 dataset [15] containing 101 MRIs as the testing datasets. To be specific, 134 structures and 50 cortical structures were manually delineated for each MRI in MALC and Mindboggle101, respectively. Finally, we randomly sampled one image from each testing dataset as the fixed image and the remaining images as the moving images to conduct the registration experiments inner each dataset. Therefore, a total of 134 pairs of registrations (34 from MALC and 100 from Mindboggle101) are used for performance evaluation.

**Preprocessing and Evaluation Metric:** We used FreeSurfer [9] to sequentially conduct the skull-stripping, affine spatial normalization, and intensity normalization for these three datasets followed by center cropping operations to resize each MRI to the dimension of  $144 \times 160 \times 192$ . Besides, we performed the histogram matching between a pre-selected image from the training dataset and the remaining 641 MRIs. Evaluation metrics including the mean of the Dice similarity coefficient (DSC), the proportion of voxels with non-positive Jacobian determinations ( $10^{-4}$ ), and their standard deviations were adopted to respectively analyze the registration accuracy and topology-preserving ability. Besides, the average running time of one registration is used to evaluate the efficiency.

#### 3.2 Results

**Compared to state-of-the-arts:** In the first set of experiments, we compared the registration results of the proposed method with some other state-of-the-art

**Table 1.** Quantitative results on mean and standard deviations of the average DSC and the proportion of voxels with non-positive Jacobian determinants ( $10^{-4}$ ), as well as the average computational time (seconds) per registration on MALC and Mindboggle101 obtained from different methods.

Methods	MALC			Mindboggle101		
	<i>Avg.DSC</i>	$ J_\phi  \leq 0$ ( $10^{-4}$ )	<i>Time</i>	<i>Avg.DSC</i>	$ J_\phi  \leq 0$ ( $10^{-4}$ )	<i>Time</i>
Affine	0.438 (0.058)	-	-	0.356 (0.017)	-	-
SyN	0.589 (0.030)	5.44 (2.95)	1443	0.549 (0.018)	1.82 (1.37)	1337
VM-diff	0.589 (0.030)	0.03 (0.03)	0.698	0.556 (0.025)	0.12 (0.13)	0.712
LapIRN	0.577 (0.027)	197.90 (42.64)	0.511	0.586 (0.017)	231.66 (33.89)	0.507
TransMorph	0.605 (0.027)	111.93 (22.05)	0.556	0.610 (0.019)	109.67 (16.53)	0.566
Ours	0.616 (0.025)	1.38 (0.95)	0.432	0.617 (0.020)	3.63 (2.69)	0.443

approaches including a typically conventional deformable image registration algorithms SyN [1] and three representatively unsupervised deformable image registration methods, diffeomorphic version of VoxelMorph (VM-diff) [7], LapIRN [20] and TransMorph [5]. NCC with a window size of 9 was adopted in  $\mathcal{S}$ , and all the other settings are configured in their default.

The statistical results derived from the application of Affine and various deformable registration approaches on MALC and Mindboggle101 datasets are presented in Table 1. Notably, our proposed method demonstrates higher registration accuracy, and the lowest running time as well as the competitive number of voxels with  $|J_\phi| \leq 0$  compared to the other four deformable registration methods on both datasets. Specifically, in comparison to the conventional registration algorithm, our method exhibits higher average DSCs on MALC (2.7%) and Mindboggle101 (6.8%). Relative to two other FCNs-based approaches, namely VM-diff and LapIRN, our method achieves a higher number of voxels with  $|J_\phi| \leq 0$  than VM-diff, yet significantly lower compared to LapIRN. While the Transformer-based registration framework exhibits superior performance compared to FCNs-based approaches in average DSCs, our proposed method surpasses it, particularly on the MALC dataset, where our method achieves 1.1% higher than TransMorph. Moreover, the topological preservation capacity of the DiffOp-net significantly outperforms it. Figure 2 illustrates coronal MRI slices obtained from moving images, fixed images, and transformed images resulting from the application of transformation fields generated by SyN, VM-diff, LapIRN, TransMorph, and DiffOp-net. It is evident from the visual examination that the aligned images produced by our proposed method exhibit the closest to the fixed images in both datasets.

**Ablation Study:** To evaluate the impact of model size on registration performance and validate the effectiveness of the CCA module proposed in our study, we conducted a second set of experiments involving the construction of three distinct models. The first two models were generated by varying the parameter  $C$  to 16 and 32, while the third model involved the removal of CCA modules from the DiffOp-net. All other configurations remained consistent with

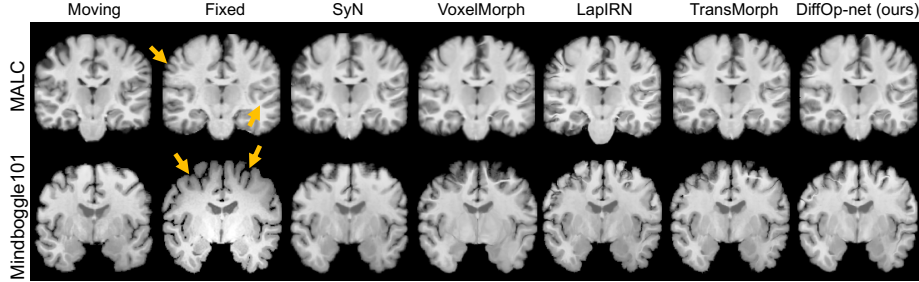


**Fig. 2.** Example MR slices of source image, fixed image and resulting deformed image from SyN, VM-diff, LapIRN, TransMorph and our method.

**Table 2.** Quantitative results on mean and standard deviations of the average DSC and the proportion of voxels with non-positive Jacobian determinants ( $10^{-4}$ ) on MALC and Mindboggle101 obtained from four models.

Methods	MALC		Mindboggle101	
	<i>Avg.DSC</i>	$ J_\phi  \leq 0$ ( $10^{-4}$ )	<i>Avg.DSC</i>	$ J_\phi  \leq 0$ ( $10^{-4}$ )
$C = 16$	0.611 (0.027)	2.57 (0.94)	0.604 (0.019)	5.02 (2.28)
$C = 32$	0.614 (0.026)	2.69 (1.18)	0.612 (0.020)	5.18 (2.57)
w/o CCA	0.612 (0.026)	3.62 (1.38)	0.610 (0.190)	5.52 (1.81)
DiffOp-net	0.616 (0.025)	1.38 (0.95)	0.617 (0.020)	3.63 (2.69)

the original DiffOp-net. The experimental results are outlined in Table 2. Upon increasing the value of  $C$  (representing model size), we observed a simultaneous improvement in accuracies for both datasets. Crucially, our proposed DiffOp-net achieved the minimal number of voxels with  $|J_\phi| \leq 0$  indicating that the optimal registration framework is achieved at  $C = 48$ . In comparison to the framework lacking CCA modules, our method exhibited superior performance, showcasing increased accuracies of 0.4% and 0.7% for the MALC and Mindboggle101, respectively. This underscores the effectiveness of the CCA module in capturing large deformations, particularly within cortical regions.

## 4 Conclusion

In this paper, we present DiffOp-net, a differential operator-based multi-resolution registration framework for velocity field prediction, to improve the performance of deformable image registration. To further effectively capture the large deformation between the image pairs, we develop a novel cross-coordinate attention module. With evaluation experiments on two datasets with different numbers of manually delineated anatomical structures, we demonstrate that our proposed model performs better than FCNs-based methods and a representative



Transformer-based method, in addition to a typical traditional algorithm. In our future work, we will adopt network architecture searching approaches to identify the optimal convolutional operations under current settings.

## References

1. Avants, B.B., Epstein, C.L., Grossman, M., Gee, J.C.: Symmetric diffeomorphic image registration with cross-correlation: evaluating automated labeling of elderly and neurodegenerative brain. *Medical image analysis* **12**(1), 26–41 (2008)
2. Balakrishnan, G., Zhao, A., Sabuncu, M.R., Guttag, J., Dalca, A.V.: Voxelmorph: a learning framework for deformable medical image registration. *IEEE transactions on medical imaging* **38**(8), 1788–1800 (2019)
3. Beg, M.F., Miller, M.I., Trounev, A., Younes, L.: Computing large deformation metric mappings via geodesic flows of diffeomorphisms. *International journal of computer vision* **61**(2), 139–157 (2005)
4. Che, T., Wang, X., Zhao, K., Zhao, Y., Zeng, D., Li, Q., Zheng, Y., Yang, N., Wang, J., Li, S.: Amnet: Adaptive multi-level network for deformable registration of 3d brain mr images. *Medical Image Analysis* **85**, 102740 (2023)
5. Chen, J., Frey, E.C., He, Y., Segars, W.P., Li, Y., Du, Y.: Transmorph: Transformer for unsupervised medical image registration. *Medical image analysis* **82**, 102615 (2022)
6. Chen, Z., Zheng, Y., Gee, J.C.: Transmatch: A transformer-based multilevel dual-stream feature matching network for unsupervised deformable image registration. *IEEE Transactions on Medical Imaging* (2023)
7. Dalca, A.V., Balakrishnan, G., Guttag, J., Sabuncu, M.R.: Unsupervised learning for fast probabilistic diffeomorphic registration. In: *International Conference on Medical Image Computing and Computer-Assisted Intervention*. pp. 729–738. Springer (2018)
8. Fan, J., Cao, X., Yap, P.T., Shen, D.: Birnet: Brain image registration using dual-supervised fully convolutional networks. *Medical image analysis* **54**, 193–206 (2019)
9. Fischl, B.: Freesurfer. *Neuroimage* **62**(2), 774–781 (2012)
10. Fu, Y., Lei, Y., Wang, T., Curran, W.J., Liu, T., Yang, X.: Deep learning in medical image registration: a review. *Physics in Medicine & Biology* **65**(20), 20TR01 (2020)
11. Hu, J., Shen, L., Sun, G.: Squeeze-and-excitation networks. In: *Proceedings of the IEEE conference on computer vision and pattern recognition*. pp. 7132–7141 (2018)
12. Hu, X., Kang, M., Huang, W., Scott, M.R., Wiest, R., Reyes, M.: Dual-stream pyramid registration network. In: *International Conference on Medical Image Computing and Computer-Assisted Intervention*. pp. 382–390. Springer (2019)
13. Jia, X., Bartlett, J., Chen, W., Song, S., Zhang, T., Cheng, X., Lu, W., Qiu, Z., Duan, J.: Fourier-net: Fast image registration with band-limited deformation. In: *Proceedings of the AAAI Conference on Artificial Intelligence*. vol. 37, pp. 1015–1023 (2023)
14. Kang, M., Hu, X., Huang, W., Scott, M.R., Reyes, M.: Dual-stream pyramid registration network. *Medical image analysis* **78**, 102379 (2022)
15. Klein, A., Tourville, J.: 101 labeled brain images and a consistent human cortical labeling protocol. *Frontiers in neuroscience* **6**, 171 (2012)
16. Landman, B., Warfield, S.: Miccai 2012 workshop on multi-atlas labeling, in: *Miccai grand challenge and workshop on multi-atlas labeling, createspace independent publishing platform, nice, france* (2012)

17. Liu, R., Li, Z., Fan, X., Zhao, C., Huang, H., Luo, Z.: Learning deformable image registration from optimization: perspective, modules, bilevel training and beyond. *IEEE Transactions on Pattern Analysis and Machine Intelligence* **44**(11), 7688–7704 (2021)
18. Liu, Y., Li, X., Li, R., Huang, S., Yang, X.: A multi-view assisted registration network for mri registration pre-and post-therapy. *Medical & Biological Engineering & Computing* pp. 1–11 (2023)
19. Mok, T.C., Chung, A.: Fast symmetric diffeomorphic image registration with convolutional neural networks. In: *Proceedings of the IEEE conference on computer vision and pattern recognition*. pp. 4644–4653 (2020)
20. Mok, T.C., Chung, A.C.: Large deformation diffeomorphic image registration with laplacian pyramid networks. In: *International Conference on Medical Image Computing and Computer-Assisted Intervention*. pp. 211–221. Springer (2020)
21. Mueller, S.G., Weiner, M.W., Thal, L.J., Petersen, R.C., Jack, C.R., Jagust, W., Trojanowski, J.Q., Toga, A.W., Beckett, L.: Ways toward an early diagnosis in alzheimer’s disease: the alzheimer’s disease neuroimaging initiative (adni). *Alzheimer’s & Dementia* **1**(1), 55–66 (2005)
22. Park, J., Woo, S., Lee, J.Y., Kweon, I.S.: Bam: Bottleneck attention module. *arXiv preprint arXiv:1807.06514* (2018)
23. Shi, J., He, Y., Kong, Y., Coatrieux, J.L., Shu, H., Yang, G., Li, S.: Xmorpher: Full transformer for deformable medical image registration via cross attention. In: *International Conference on Medical Image Computing and Computer-Assisted Intervention*. pp. 217–226. Springer (2022)
24. Tang, X., Qin, Y., Wu, J., Zhang, M., Zhu, W., Miller, M.I.: Shape and diffusion tensor imaging based integrative analysis of the hippocampus and the amygdala in alzheimer’s disease. *Magnetic resonance imaging* **34**(8), 1087–1099 (2016)
25. Tian, L., Greer, H., Vialard, F.X., Kwitt, R., Estépar, R.S.J., Rushmore, R.J., Makris, N., Bouix, S., Niethammer, M.: Gradicon: Approximate diffeomorphisms via gradient inverse consistency. In: *Proceedings of the IEEE conference on computer vision and pattern recognition*. pp. 18084–18094 (2023)
26. Vercauteren, T., Pennec, X., Perchant, A., Ayache, N.: Diffeomorphic demons: Efficient non-parametric image registration. *NeuroImage* **45**(1), S61–S72 (2009)
27. Woo, S., Park, J., Lee, J.Y., Kweon, I.S.: Cbam: Convolutional block attention module. In: *Proceedings of the European conference on computer vision (ECCV)*. pp. 3–19 (2018)
28. Wu, J., Tang, X.: A large deformation diffeomorphic framework for fast brain image registration via parallel computing and optimization. *Neuroinformatics* pp. 1–16 (2019)
29. Yang, S.D., Zhao, Y.Q., Zhang, F., Liao, M., Yang, Z., Wang, Y.J., Yu, L.L.: An abdominal registration technology for integration of nanomaterial imaging-aided diagnosis and treatment. *Journal of Biomedical Nanotechnology* **17**(5), 952–959 (2021)
30. Yang, X., Kwitt, R., Styner, M., Niethammer, M.: Quicksilver: Fast predictive image registration—a deep learning approach. *NeuroImage* **158**, 378–396 (2017)
31. Zhang, M., Fletcher, P.T.: Fast diffeomorphic image registration via fourier-approximated lie algebras. *International Journal of Computer Vision* **127**, 61–73 (2019)